Available online at www.sciencedirect.com
SciVerse ScienceDirect
Ceramics International 38 (2012) 5557–5561
CERAMICS INTERNATIONAL
www.elsevier.com/locate/ceramint

Crystal plane evolution of grain oriented alumina ceramics with high transparency

Hailan Yi [a,b], Xiaojian Mao [a], Guohong Zhou [a], Shi Chen [a], Xiaoqing Zou [a,b], Shiwei Wang [a,*], Shunzo Shimai [a]

[a] *Shanghai Institute of Ceramics, Chinese Academy of Sciences, Shanghai 200050, China*
[b] *Graduate School of Chinese Academy of Science, Beijing 100039, China*

Received 22 September 2011; received in revised form 26 March 2012; accepted 29 March 2012
Available online 5 April 2012

Abstract

Transparent alumina ceramics with oriented grains were successfully prepared by slip casting under an assisted magnetic field and sintering at 1850 °C for 5 h in vacuum. In-line transmittance of the alumina ceramic shaped under 12 T reaches as high as 70.3% at 600 nm. Detailed crystal plane evolution of grain oriented alumina ceramics with the assistance of different magnitude magnetic field was studied by XRD characterization. The results indicate that complete textured structure could only be realized with a magnetic field strength above 12 T. Furthermore, the grain microstructure was observed by optical microscope in different directions.

Keywords: A. Slip casting; A. Sintering; Transparent alumina; Grain orientation; Crystal plane

1. Introduction

Alumina ceramics have been widely investigated and used due to their good mechanical, chemical, thermal, optical and other considerable properties since the middle of last century [1–7]. Since then, great efforts [8] have been made to prepare alumina ceramics with those desirable properties [2,9]. Recently, researches on controlled highly textured alumina have been reported by Sakka et al. [10], Uematsu et al. [11,12], Zhang et al. [13]. High orientation of alumina grains was accomplished by applying a strong magnetic field to the suspension of alumina powder during the colloidal shaping process, and sintering at about 1600 °C in air. More recently, Mao et al. [14] prepared transparent polycrystalline alumina ceramics with optical axes using a similar magnetic field assisted texturing method [10], followed by sintering at 1850 °C in H_2 atmosphere. The reported transparent alumina showed remarkably higher transmittance (55% at 600 nm) than that of conventional translucent alumina ceramics with a fully random oriented grain structure. Furthermore, its in-line transmittance in ultra-violet region remained a high value [14]. It seems that double refraction was minimized in the transparent alumina ceramics prepared with the assistance of a strong magnetic filed.

However, the transmittance of the grain oriented alumina ceramic is still far from that of sapphire; the microstructure and crystal plane evolution mechanism have not been studied in detailed in the previous report [14]. The aim of this work is to fabricate grain oriented transparent alumina with enhanced in-line transmittance by optimizing slip casting with assisted different magnitude magnetic field, and sintering at 1850 °C in vacuum. The influence of magnetic field strength on the grain orientation degree as well as the evolution of crystal plane was demonstrated.

2. Experimental procedure

High quality α-alumina powder (Sumitomo Chemical Co., Ltd., Japan) with a purity of 99.99%, a mean particle size about 400 nm and a BET specific surface area about 6 m^2/g, was selected as raw material. 400 ppm MgO was added as a sintering aid. Alumina suspension with about 25 vol% solids was prepared by mixing the raw powders with polyacrylate ammonium (DISPEX A40, CIBA Co., Switzerland), and

* Corresponding author.
E-mail address: swwang51@mail.sic.ac.cn (S. Wang).

0272-8842/$36.00
http://dx.doi.org/10.1016/j.ceramint.2012.03.074

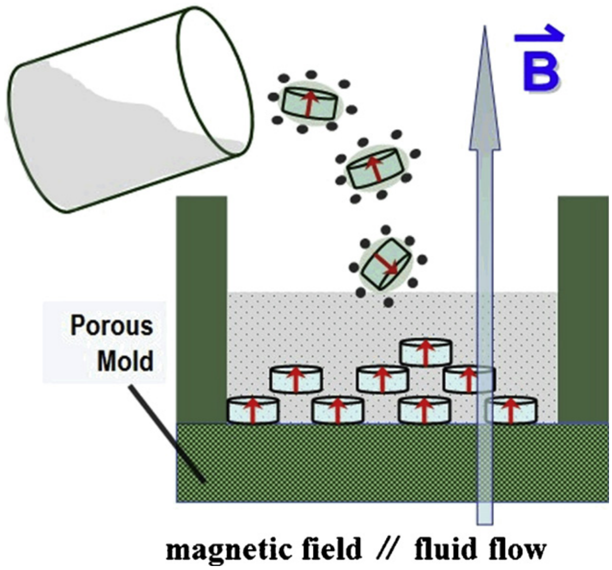

Fig. 1. Schematic diagram of slip casting under magnetic field.

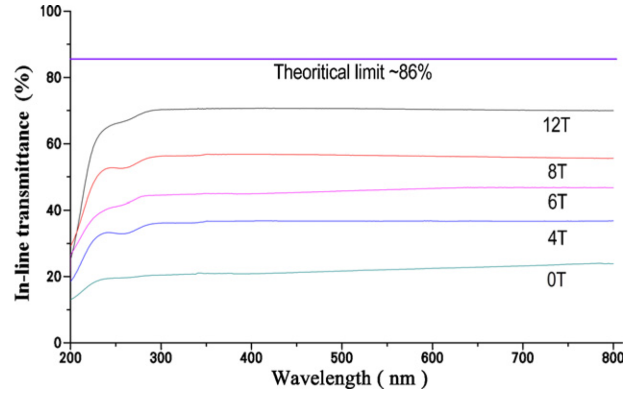

Fig. 2. In-line transmittance of alumina ceramics (1 mm thick) slip-casted under magnetic field and then sintered at 1850 °C for 5 h in vacuum.

deionized water, using ultrasonic dispersion for 30 min and planetary ball milling for 10 h.

Slip casting process was carried out using the resultant alumina suspension with the presence of magnetic field (12/14/98 Magnetic Field Instrument, Oxford Instruments plc, UK) where the magnetic field direction was parallel to the casting direction, as shown in Fig. 1. The strength of magnetic field will be adjusted to be 0 T (random grain oriented) to 12 T. After casting, the wet green bodies were dried at 120 °C for 24 h and calcined at 800 °C for 2 h in air. The final densification of ceramics was carried out by pressureless sintering at 1850 °C for 5 h in vacuum with the vacuum level around 2×10^{-3} Pa.

In order to analyze the quantitative orientation, the ceramics were characterized by X-ray diffraction (Model D/MAX-2550V, Rigaku Industrial Co., Osaka, Japan) using a $\theta/2\theta$ pattern on the testing slices which were cut horizontally (perpendicular to the magnetic field direction) and vertically (parallel to the magnetic field direction) from the ceramics, noted as top and side slices, respectively.

For the measurement of in-line transmittance, the obtained ceramics were polished on both sides to a thickness of 1 mm. An UV-VIS-NIR spectrophotometer (Cary 5000, Varian Inc., USA) was employed. Optical microscope (Olympus Co., Japan) was used to observe the microstructure of the top and side slices.

3. Results and discussion

3.1. In-line transmittance of alumina ceramics

Fig. 2 shows the in-line transmittance of these polished alumina ceramics. It is obviously the in-line transmittances of the alumina ceramics shaped under magnetic field are much higher than that of the grain random oriented alumina shaped under 0 T (without magnetic field). With the increase of strength of magnetic field, in-line transmittance of the ceramics is enhanced accordingly. The sample shaped under 12 T shows the highest in-line transmittance, which is equal to 70.3% at 600 nm, 81.7% of the theoretical transmittance limit (~86%). The transmittance remains relatively a high level as the wavelength shifted towards the short-wavelength range, for example, ~70% at 300 nm. Furthermore, the in-line transmittance curves of the alumina ceramics shaped under magnetic field are similar to that of transparent ceramics with cubic crystal structure. These results imply that the influence of double refraction of alumina ceramics on in-line transmittance could be minimized, or even eliminated, with the sufficient texturing of crystal planes, resulting an excellent transparence from UV to visible region for the sintered alumina ceramics.

To get a more visual comparison, photos of alumina ceramics shaped under 12 T (oriented grain) and without magnetic field (random oriented grain) are shown in Fig. 3. The samples shown in Fig. 3a and b were placed 15 mm above the printed letters, while the distance between buildings and the sample in Fig. 3c is farther than 90 m. It is obvious that the alumina ceramics shaped under 12 T shows excellent transparency. However, the alumina ceramics shaped without magnetic field in Fig. 3b is merely translucent. Because α-alumina is a trigonal and uniaxial structure, optically uniaxial and birefringent, with an optical birefringence index of 0.008 at 600 nm, light birefraction which occurs repetitively when light passing through numerous random oriented grains results in the blurred vision of the printed letters (Fig. 3b).

3.2. Evolution of crystal planes

All XRD patterns of the ceramics shaped under different magnetic fields are illustrated in Fig. 4 (top slices) and Fig. 5 (side slices). For the ceramics shaped without magnetic field, all diffractive peaks of alumina appear on both top and side slices, revealing a microstructure of typical traditional α-alumina, i.e. random aligned grain structure. However, fewer diffractive peaks are found on XRD patterns in Figs. 4 and 5 when the magnetic field was utilized. This result clearly demonstrates the magnetic field induced orientation occurrence because the magnetic crystal anisotropy energy is larger than thermal motion energy [15–18].

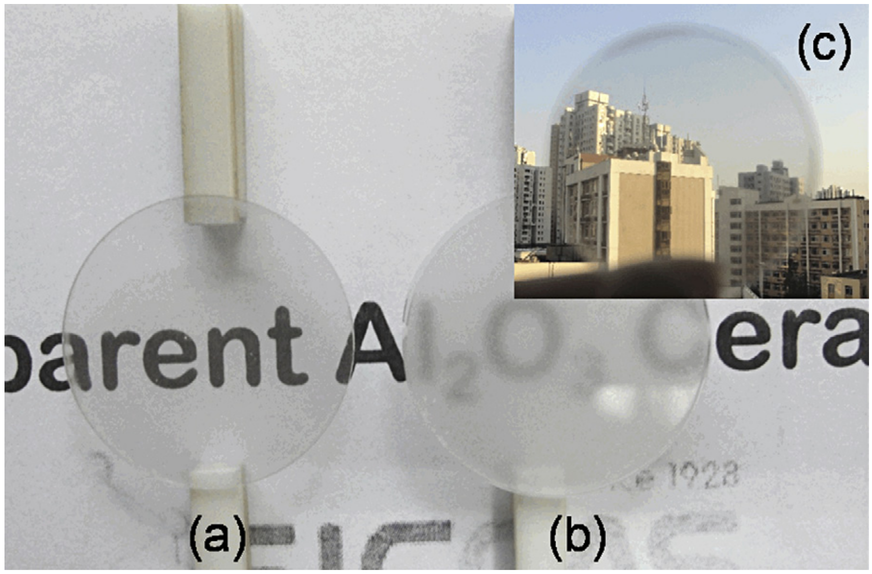

Fig. 3. Polycrystalline alumina ceramics slip-cast under (a, c) 12 T and (b) 0 T followed by sintering at 1850 °C for 5 h in vacuum.

For XRD patterns of top slices in Fig. 4, the diffraction intensity of peaks (006) related to *c*-planes (00*l*) is enhanced when the strength of magnetic field increased. When the ceramics were shaped under 4 T, several XRD diffraction peaks disappear, such as (012), (110), (024), (214) and (300). But the planes nearly parallel to *c*-planes with relatively low interplanar angles remain present on XRD pattern of top slice (Fig. 4, 4 T), such as (104), (116), (018), (10<u>10</u>) planes with an angle of 38.25°, 42.3°, 21.5°, 17.5°, respectively. As the magnetic field strength approached to 6 T and 8 T, only those diffraction peaks with even lower interplanar angles, such as (10<u>10</u>) and (018), appear on the patterns. For top slice of the ceramics shaped under 12 T, the existing diffraction peak is only *c*-plane (006), which distinctly indicates that alumina prepared under 12 T exhibits thorough grain orientation along the direction of *c*-axes and magnetic field.

For XRD patterns of side slices in Fig. 5, the diffraction intensities of (*hk*0) planes perpendicular to *c*-planes, such as (110) and (300) planes, are enhanced with the increase of the magnetic field strength. When alumina ceramics was shaped under 4 T, several XRD diffraction peaks disappear, such as (104), (116), (018), and (10<u>10</u>), though these peaks remain for top slices (Fig. 4, 4 T). However, the planes nearly perpendicular to *c*-planes with relatively larger interplanar angles still appear for side slices (Fig. 5, 4 T), such as (012), (113) with an angle of 57.6°, 61.2°. With the magnetic field strength raising to 6 T, 8 T and 12 T, only the diffraction peaks perpendicular to *c*-plane are found for side slices, such as (300) and (110). The XRD characterization demonstrates that a complete crystalline texture with the *c*-axis parallel to the direction of magnetic field is obtained by slip-casting within a high assisted magnetic field and sintering. In other words, alumina ceramics fabricated via magnetic alignment method provides grains with *c*-axis parallel to each other and to the optical axis. Therefore, when light transmits through optical axis of grains, the physical environment remains the same; theoretically birefringence of the grain boundary can be eliminated. This is why in-line transmittance of the ceramics we prepared is greatly improved (Fig. 2).

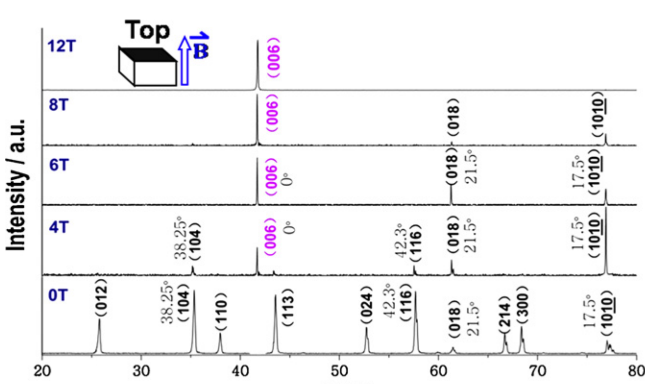

Fig. 4. XRD patterns of top slices of alumina ceramics shaped under 0 T, 4 T, 6 T, 8 T, 12 T magnetic fields, respectively.

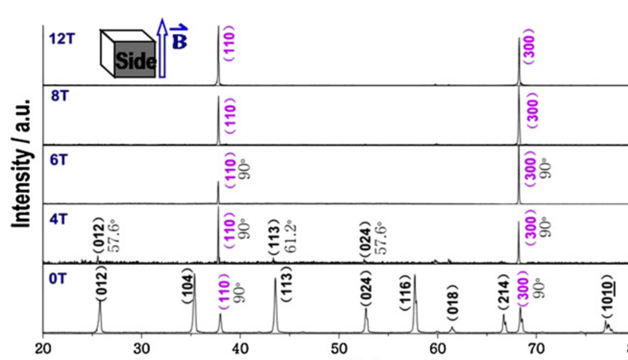

Fig. 5. XRD patterns of side slices of alumina ceramics shaped under 0 T, 4 T, 6 T, 8 T, 12 T magnetic fields, respectively.

Table 1
Orientation factor and in-line transmittance of alumina ceramics shaped under magnetic field.

Magnetic strength	0 T	4 T	6 T	8 T	12 T
In-line transmission at 600 nm (%)	22.5	36.8	46.5	58.2	70.3
c-axes, $f_{(006)}$	~0	0.24	0.52	0.78	0.97

3.3. Magnetic field strength versus grain orientation degree

There are several ways to describe the orientation degree of textured materials [11,19,20]. Lotgering orienting factor *f* from the $\theta/2\theta$ mode of XRD measurements is generally used as a semi-quantitative, but straightforward way.

Based on the XRD spectra, the orientation factor *f* is calculated according to definition equation (1):

$$f = \frac{P_s - P_0}{1 - P_0} \quad (1)$$

For *c*-axis orientation:

$$P_s \text{ and } P_0 = \frac{\sum I_{00l}}{\sum I_{hkl}}$$

where $\sum I_{(00l)}$ is the sum of peak intensities of the (00*l*) planes perpendicular to *c*-axis of α-alumina crystal, and $\sum I_{(hkl)}$ is the sum of peak intensities of all the (*hkl*) planes in the range of 2θ. The values of P_s are obtained from XRD patterns of the sample slices, and P_0 is calculated from standard α-alumina (JCPDS card No. 43-1484). For the grain fully random oriented sample, *f* equals zero, while for single crystal, *f* equals 1. The absolute value of *f* increases with the increasing degree of orientation.

Table 1 illustrates the calculated data of the orientation factor *f* based on XRD patterns (Fig. 4) of transparent alumina ceramics, which are prepared by slip casting under magnetic field and sintering at 1850 °C for 5 h in vacuum. The in-line transmittances of the alumina ceramics at 600 nm are also presented in Table 1. Both *f* value and in-line transmittance increase with the escalating of magnetic field strength. In other words, alumina ceramics with better orientation results in higher in-line transmittance.

Fig. 6 shows microstructures of the polished and thermal etched surfaces of transparent alumina ceramics, which are shaped under 12 T and sintered at 1850 °C for 5 h in vacuum. For the top slice, the grains appear to be nearly isometric shape as shown in Fig. 6a, and the grain size is ~40 μm. In contrast, most grains on the side slice in Fig. 6b show nearly lath-shaped. This indicates that platelet grains align perpendicular to the magnetic field are obtained.

Grain oriented alumina shows much higher transmittance than that of traditional polycrystalline alumina, so it is an effective way to preparing highly transmitting alumina ceramics by strong magnetic field assisted slip casting and sintering. The in-line transmittance of obtained samples is not so high as sapphire, the main reasons should be as below: incompletely oriented grains; the scattering of lights due to the grain boundaries and few pores inside samples. So microstructure of the transparent alumina ceramics could be further optimized to improve the in-line transmittance of alumina ceramics.

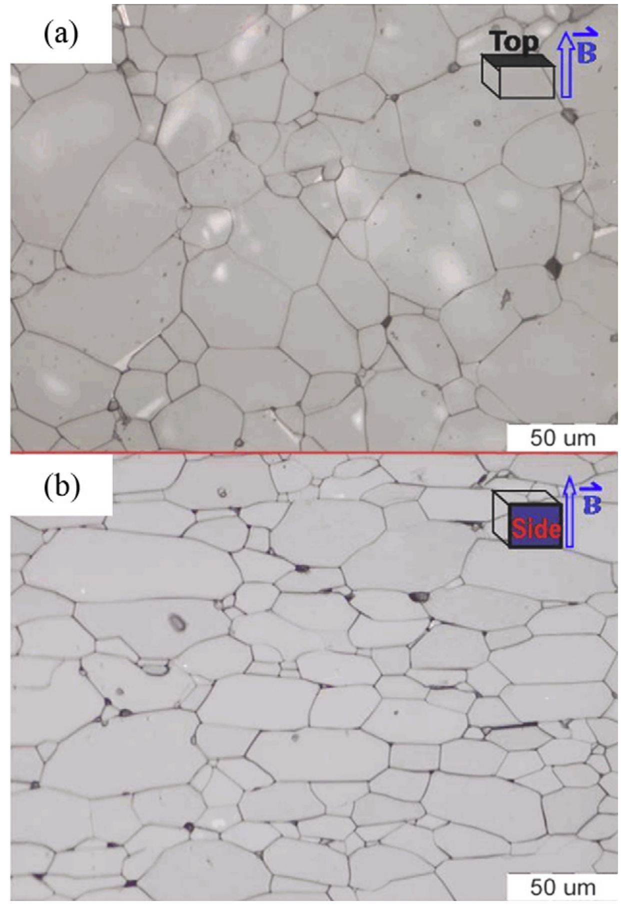

Fig. 6. Thermal etched surfaces of transparent ceramics shaped under 12 T and subsequent sintered at 1850 °C, (a) top slice, (b) side slice.

4. Conclusions

(1) Transparent alumina ceramics with thoroughly oriented grains were successfully prepared by slip casting under a 12 T magnetic field and sintering at 1850 °C for 5 h in vacuum. The in-line transmittance is 70.3% at 600 nm, 81.7% of the theoretical limit.
(2) XRD patterns of the top surfaces perpendicular to the direction of magnetic field show that with the increase of magnetic field strength, planes with relatively larger interplanar angles to *c*-planes disappear first, and then those with lower interplanar angles vanished; finally only the (00*l*) planes are present on the pattern. Contrarily, for the side slices, planes with relatively lower angles to *c*-planes disappear first, and then only the (*hk*0) planes exist.
(3) Both orientation factor $f_{(006)}$ and in-line transmittance are enhanced with the increase of magnetic field strength. Microstructure observation reveals that platelet grains are aligned perpendicular to the magnetic field.

Acknowledgment

This work is financially supported by China National 863 Project (2009AA03Z440).

References

[1] R.L. Coble, Transparent Alumina and Method of Preparation, U.S. Patent No. 3,026,210, 1962.
[2] B.N. Kim, K. Hiraga, K. Morita, H. Yoshida, Effects of heating rate on microstructure and transparency of spark-plasma-sintered alumina, Journal of the European Ceramic Society 29 (2) (2009) 323–327.
[3] T.Y. Chan, S.J. Liu, S.T. Lin, Effects of high concentrations of liquid phase and magnesia on the grain growth of alumina, Ceramics International 24 (8) (1998) 617–625.
[4] M. Shan, X.J. Mao, J. Zhang, S.W. Wang, Electrophoretic shaping of submicron alumina in ethanol, Ceramics International 35 (5) (2009) 1855–1861.
[5] A. Krell, G. Baur, C. Dahne, Transparent sintered Sub-μm Al_2O_3 with IR transmissivity equal to sapphire, Proceedings of SPIE 5078 (2003) 199–207.
[6] A. Krell, P. Blank, H.W. Ma, T. Hutzler, M.P.B. van Bruggen, R. Apetz, Transparent sintered corundum with high hardness and strength, Journal of the American Ceramic Society 86 (1) (2003) 12–18.
[7] G.C. Wei, Transparent ceramic lamp envelope materials, Journal of Physics D – Applied Physics 38 (17) (2005) 3057–3065.
[8] C. Scott, M. Kaliszewski, C. Greskovich, L. Levinson, Conversion of polycrystalline alumina into single-crystal sapphire by abnormal grain growth, Journal of the American Ceramic Society 85 (5) (2002) 1275–1280.
[9] R. Apetz, M.P.B. van Bruggen, Transparent alumina: a light-scattering model, Journal of the American Ceramic Society 86 (3) (2003) 480–486.
[10] T.S. Suzuki, Y. Sakka, K. Kitazawa, Orientation amplification of alumina by colloidal filtration in a strong magnetic field and sintering, Advanced Engineering Materials 3 (7) (2001) 490–492.
[11] A. Makiya, S. Tanaka, D. Shoji, T. Ishikawa, N. Uchida, K. Uematsu, A quantitative evaluation method for particle orientation structure in alumina powder compacts, Journal of the European Ceramic Society 27 (12) (2007) 3399–3406.
[12] T. Takenaka, K. Sakata, Grain orientation and electrical properties of hot-forged $Bi_4Ti_3O_{12}$ ceramics, Japanese Journal of Applied Physics 19 (1) (1980) 31–39.
[13] L. Zhang, J. Vleugels, O. Van der Biest, Slip casting of alumina suspensions in a strong magnetic field, Journal of the American Ceramic Society 93 (10) (2010) 3148–3152.
[14] X.J. Mao, S.W. Wang, S. Shimai, J.K. Guo, Transparent polycrystalline alumina ceramics with optical axes, Journal of the American Ceramic Society 91 (10) (2008) 3431–3433.
[15] T. Sugiyama, M. Tahashi, K. Sassa, S. Asai, The control of crystal orientation in non-magnetic metals by imposition of a high magnetic field, ISIJ International 43 (6) (2003) 855–861.
[16] S. Asai, Application of high magnetic fields in inorganic materials processing, Modelling and Simulation in Materials Science and Engineering 12 (2) (2004) R1–R12.
[17] T.S. Suzuki, T. Uchikoshi, Y. Sakka, Control of texture in alumina by colloidal processing in a strong magnetic field, Science and Technology of Advanced Materials 7 (2006) 356–364.
[18] T.S. Suzuki, Y. Sakka, Control of texture in electroceramics by slip-casting in a high magnetic field, Key Engineering Materials 248 (2003) 191–194.
[19] E. Guilmeau, C. Henrist, T.S. Suzuki, Y. Sakka, D. Chateigner, D. Grossin, B. Ouladdiaf, Texture of alumina by neutron diffraction and SEM-EBSD, Icotom 14: Textures of Materials 495–497 (Pts 1and 2) (2005) 1395–1400.
[20] X.W. Zhu, Y. Sakka, Textured silicon nitride: processing and anisotropic properties, Science and Technology of Advanced Materials 9 (3) (2008) 47.